View Article Online / Journal Homepage / Table of Contents for this issue
Dynamic Article Links

NJC

Cite this: *New J. Chem.*, 2011, **35**, 2793–2803

www.rsc.org/njc

PAPER

Tetrahalidocuprates(II)—structure and EPR spectroscopy. Part 1:† Tetrabromidocuprates(II)‡

Ramzi Farra,[ab] Kerstin Thiel,[ac] Alette Winter,[a] Tillmann Klamroth,[a] Andreas Pöppl,[d] Alexandra Kelling,[a] Uwe Schilde,[a] Andreas Taubert[ae] and Peter Strauch*[a]

Received (in Montpellier, France) 24th March 2011, Accepted 13th September 2011
DOI: 10.1039/c1nj20271e

Tetrahalidocuprates(II) show a high degree of structural flexibility. We present the results of crystallographic and electron paramagnetic resonance (EPR) spectroscopic analyses of four new tetrabromidocuprate(II) compounds and compare the results with previously reported data. The cations in the new compounds are the sterically demanding benzyltriphenylphosphonium, methyltriphenylphosphonium, tetraphenylphosphonium, and hexadecyltrimethylammonium ions; they were used to achieve a reasonable separation of the paramagnetic Cu(II) ions for EPR spectroscopy. X-Ray crystallography shows that in all four complexes the $[CuBr_4]^{2-}$ units have a distorted tetrahedral coordination geometry which is in agreement with DFT calculations. The EPR hyperfine structure was not resolved. This is due to the exchange broadening resulting from still incomplete separation of the paramagnetic Cu(II) centres. Nevertheless, the principal values of the electron Zeemann tensor ($g_{||}$ and $g_{\perp}$) of the complexes could be determined. A correlation of structural (X-ray) parameters with the spin density at the copper centres (DFT) is well reflected in the EPR spectra of the bromidocuprates. This enables the correlation of X-ray and EPR parameters to predict the structure of tetrabromidocuprates in physical states other than the crystalline state. As a result, we provide a method to structurally characterize $[CuBr_4]^{2-}$ in, for example, ionic liquids or in solution, which has important implications for *e.g.* catalysis or materials science.

Introduction

Tetrahalidocuprate complexes $A_2[CuX_4]$ (X = Cl^-, Br^-) have been known for a long time and several authors[1–5] have reported a remarkable variety of the counter cations (A) in halidocuprate(II) complexes. Cations range from simple inorganic cations (Li^+, Cs^+, Rb^+, NH_4^+)[6–9] to complex inorganic[4,5,10] and complex organic cations[11–14] such as substituted ammonium, phosphonium, pyridinium, imidazolium, and pyrrolidinium.

The first crystal structure of a tetrahalidocuprate(II), $Cs_2[CuCl_4]$, was reported in 1952 by L. Helmholz and R. F. Kruh.[1] Tetrahalidocuprates(II) with large organic cations of the type $[As(C_6H_5)_3CH_3]_2[CuX_4]$ were first prepared by N. S. Gill and R. S. Nyholm.[2] They have also shown a distortion from the discrete tetrahedral geometry. Indeed the $[CuX_4]^{2-}$ moiety exhibits a remarkable flexibility in coordination geometry between square planar and nearly perfect tetrahedral. The fact that tetrahalidocuprates(II) change their degree of distortion in dependence of the structure of the counter-cations makes them interesting for research and technology, because the physical and chemical properties of the corresponding complexes will be altered as the bond angles in the tetrahalidocuprate anion change. Tetrahalidocuprates have attracted attention for their wide range of applications, such as catalysis, and for their interesting and flexible structural features in the liquid and the solid state, which strongly depend on the counter-cation.

R. D. Willett *et al.*[15] reported one of the most striking properties of the tetrachloridocuprates(II), thermochromism, which is interpreted as a phase transition accompanied by a change in the coordination geometry from square planar to distorted tetrahedral with increasing temperature. These phase transitions are characterized by colour changes from green to

[a] *University of Potsdam, Institute of Chemistry, Karl-Liebknecht-Str. 24-25, D-14476 Potsdam/Golm, Germany. E-mail: pstrauch@uni-potsdam.de*
[b] *Fritz-Haber-Institute, Department of Inorganic Chemistry, Faradayweg 4-6, D-14195 Berlin, Germany*
[c] *Technical University of Berlin, Institute of Chemistry, Englische Strasse 20, D-10587 Berlin, Germany*
[d] *University of Leipzig, Institute of Experimental Physics, Linnéstr. 5, D-04103 Leipzig, Germany*
[e] *Max Planck Institute of Colloids and Interfaces, Am Mühlenberg 1, D-14476 Potsdam/Golm, Germany*

† Part 2 will deal with the tetrachloridocuprate(II) complexes.

‡ Electronic supplementary information (ESI) available: CCDC reference numbers 818359 (**1**), 818358 (**2**), 818357 (**3**) and 818356 (**4**). For ESI and crystallographic data in CIF or other electronic format see DOI: 10.1039/c1nj20271e

Published on 05 October 2011. Downloaded by TU Berlin - Universitaetsbibl on 31/03/2016 12:42:47.

View Article Online

Published on 05 October 2011. Downloaded by TU Berlin - Universitaetsbibl on 31/03/2016 12:42:47.

yellow in chloridocuprate(II) and from green to violet in bromidocuprate(II) complexes.[8,15–18] Moreover, the magnetism and magnetochromism of tetrabromidocuprates(II) was recently analyzed by J. D. Woodward *et al.*[19–21] Tetrabromidocuprates have also been used as interesting building blocks for magnetic materials *e.g.* spin-ladder materials or layered structures by C. P. Landee, J. J. Novoa, M. M. Turnbull *et al.*[22–26] Finally, tetrahalidocuprate(II) complexes have been used as catalysts or catalyst precursors.[27,28]

Liquid crystalline ionic liquids on the basis of tetrahalidometalates (M = Co, Ni) have been reported first in 1996 by C. J. Bowlas, D. W. Bruce and K. R. Seddon.[29] F. Neve *et al.*[30–33] have shown that tetrahalidocuprate(II) complexes based on alkylpyridinium cations with an alkyl chain length of $n \geq 12$ are thermotropic liquid crystals. With shorter alkyl chains they are ionic liquids (ILs). Moreover, alkylpyridinium tetrahalidocuprate ILs and ionic liquid crystals (ILCs) have also been used as precursors for inorganic materials.[34–36] Reports on tetrahalidometalate-based ILCs and their transformation into inorganic materials are, however, relatively rare.[30–33,37–47] This is somewhat surprising because metal containing ILs and ILCs may open the door towards a new valuable branch of IL research, which derives its importance from the additional properties such as colour, geometry, or magnetism, which are brought about the material by the metal ion.

In 1997 R. Hoffmann[48] stated that "there is no more basic enterprise in chemistry than the determination of the geometrical structure of a molecule. Such a determination, when it is well done, ends speculation and provides us with the starting point for the understanding of every physical, chemical, and biological property of the molecule". Indeed, there were many attempts to correlate the degree of distortion of tetrahalidocuprate(II) complexes with their spectral parameters using UV-vis,[49,50] and EPR[51] spectroscopy, or other methods.[4,20,52,53] EPR spectroscopy in particular is highly suitable for the investigation of Cu(II) compounds because of its high sensitivity towards paramagnetic systems and the possibility to investigate the samples in various physical states, *i.e.*, liquids and solids (powder, single crystal, and frozen solution). It is therefore possible to study the structure of a complex such as the tetrahalidocuprate(II) and its electronic configuration under a variety of conditions. This provides access to complementary information, which is often not accessible from one experiment (or physical state) alone.

Moreover, the investigation of dynamic systems like tetrahalidocuprate(II) complexes in ILs is possible as well. As a result, some tetrahalidocuprate(II) complexes were already examined by EPR spectroscopy.[9,54–58] The recent past has seen an increasing interest in halidocuprate(II) and EPR spectroscopy investigations supported by X-ray structure determination on doped crystals,[59] powders of single crystals with different and somewhat sterically demanding cations,[60–64] and single crystals.[65] Compared to chloridocuprate(II) complexes, there is currently relatively little knowledge on the bromide complexes. We have therefore synthesised a new series of bromidocuprates(II) and characterized them predominantly with X-ray diffraction, EPR spectroscopy, and extensive comparison with published data. The goal of this study is the correlation of experimental EPR parameters with the degree of distortion θ in the $[CuBr_4]^{2-}$ moieties in order to answer the question: To which extent is it possible to predict or extract the structure of tetrabromidocuprates(II) from EPR parameters? The practical implication of this work is that, if there is indeed a structure–EPR parameter correlation, it should be possible to determine (or at least estimate) the structure of tetrahalidocuprates(II) in the amorphous or liquid state. Among others, this is of importance to IL research and technology, where the physical parameters are not always easily related to a chemical or supramolecular structure.[66]

Experimental

Chemicals

The following chemicals were used without further purification: copper(II) bromide (99%, Alfa Aesar), hydrogen bromide (47 wt%, Merck), chloroform (VWR/Prolabo, recatpur, ≥ 99%), ethanol anhydrous (99%, Berkel AHK), potassium bromide (Uvasol, for IR-spectroscopy, Merck), methyltriphenylphosphonium bromide (98%, Merck), tetraphenylphosphonium bromide (97%, Aldrich), hexadecyltrimethylammonium bromide (98%, Fluka), benzyltriphenylphosphonium bromide (99%, Aldrich), *n*-hexane (96%, Riedel-de Haen), and diisopropyl ether (100%, Ferale).

Preparation

The synthesis of tetrabromidocuprate(II) complexes can be accomplished either (1) by first preparing the internal $[CuBr_4]^{2-}$ coordination sphere followed by addition of the counter ion as bromide salt or (2) by preparation of the internal coordination sphere *in situ* by adding an ethanolic solution of $CuBr_2$ to an excess amount of the bromide salt of the counter ion dissolved in a minimum volume of ethanol. We have to mention here that the excess amount of the bromide salt could be replaced by using a concentrated aqueous solution of HBr, and the presence of this excess of Br^- ions in the solution ensures the formation of tetrabromidocuprate(II) moiety on one side and prevents solvolysis on the other side.[67]

In the current work, the $[CuBr_4]^{2-}$ moiety was synthesized according to a protocol by H. Liu *et al.*[68] 0.03 mol (6.7 g) of $CuBr_2$ were dissolved in 25.5 mL of aqueous HBr (47%wt) and the mixture was heated in a flask with a reflux condenser for 30 minutes to 70 °C. After cooling a dark purple solution was obtained. This solution was directly used for the preparation of complex **1**.

Bis(benzyltriphenylphosphonium)tetrabromidocuprate(II), $(BzlPh_3P)_2[CuBr_4]$ (1). For complex **1** 0.002 mol (0.9 g) of benzyltriphenylphosphonium bromide were dissolved in 15 mL of $CHCl_3$. Subsequently, 2 mL of the dark purple tetrabromidocuprate solution were slowly added to the benzyltriphenylphosphonium bromide solution. Two coloured phases were formed from where the organic solvent (chloroform) was slowly evaporated at atmospheric pressure and 40 °C. Dark violet micro-crystalline powder was obtained and separated by filtration.

Melting point: 141–142 °C; yield 1.96 g (90%). Elemental analysis calculated for $(BzlPh_3P)_2[CuBr_4]\cdot 2CHCl_3$, $C_{50}H_{44}P_2CuBr_4\cdot 2CHCl_3$

 This journal is © The Royal Society of Chemistry and the Centre National de la Recherche Scientifique 2011

View Article Online

Published on 05 October 2011. Downloaded by TU Berlin - Universitaetsbibl on 31/03/2016 12:42:47.

(1328.68): C 47.11, H 3.43 (%); found: C 46.96, H 3.46 (%). Main IR-bands (KBr, cm^{-1}): 3055m $\nu(sp^2$ C–H), 2963m $\nu_{symmetric}$ (sp^3 C–H), 2881m $\nu_{asymmetric}$ (sp^3 C–H), 1584m, 1483m, 1436s, 1317m ν(C–C), 1188δ(C–H), 1163m, 1110s ν(C–P), 996m, 787m, 749s, 718s γ(C–H), 691s ν(C–C).

Bis(methyltriphenylphosphonium)tetrabromidocuprate(II), $(MePh_3P)_2[CuBr_4]$ (2). The following complexes were prepared according to the second approach briefly mentioned above following published procedures.[69] 0.004 mol (500 mg) of copper(II) bromide, previously dissolved in 10 mL of ethanol, were added slowly to 0.01 mol (3.2 g) of methyltriphenylphosphonium bromide dissolved in a minimum volume of ethanol (5 mL). After a while the complex precipitated as dark purple polycrystalline powder.

Melting point: 129 °C; yield 3.2 g (86%). Elemental analysis calculated for $(MePh_3P)_2[CuBr_4]$, $C_{38}H_{36}P_2CuBr_4$ (937,81): C 48.61, H 3.691 (%); found: C 48.66, H 3.87 (%). Main IR-bands (KBr, cm^{-1}): 3053m $\nu(sp^2$ C–H), 2963m $\nu_{symmetric}$ (sp^3 C–H), 2898m $\nu_{asymmetric}$ (sp^3 C–H), 1584m, 1481m, 1436s, 1321m ν(C–C), 1188 δ(C–H), 1160m, 1113s ν(C–P), 995m, 899s, 886s, 748s, 717s γ(C–H), 688s ν(C–C).

Bis(tetraphenylphosphonium)tetrabromidocuprate(II), $(Ph_4P)_2[CuBr_4]$ (3). The other complexes were prepared *via* the same protocol as for $(MePh_3P)_2[CuBr_4]$ using the following quantities: 0.004 mol (500 mg) $CuBr_2$ dissolved in 10 mL of ethanol and 0.01 mol (3.5 g) tetraphenylphosphonium bromide dissolved in 11 mL of ethanol.

Melting point: 186–190 °C; yield 3.8 g (89%). Elemental analysis calculated for $(Ph_4P)_2[CuBr_4]$, $C_{48}H_{40}P_2CuBr_4$ (1061.96): C 54.27, H 3.60 (%); found: C 54.28, H 3.79 (%); IR (KBr, cm^{-1}): 3056m $\nu(sp^2$ C–H), 1584m, 1481m, 1436s, 1337w ν(C–C), 1183 δ(C–H), 1160w, 1107s ν(C–P), 996m, 756m, 722s γ(C–H), 688s ν(C–C).

Bis(hexadecyltrimethylammonium)tetrabromidocuprate(II), $(Me_3C_{16}N)_2[CuBr_4]$ (4). This complex was synthesized by the same protocol as compound **1** with the following quantities: 3.64 g (0.01 mol) of hexadecyltrimethylammonium bromide were dissolved in 15 mL of chloroform and 2 mL of a concentrated tetrabromidocuprate(II) solution as described above. The mixture was stirred for about 10 minutes, after that a dark purple solution separates into two phases. The purple chloroform phase was separated and evaporated to dryness. The dark purple crystals are soluble in water and in polar solvents. They are stable at room temperature.

Melting point: 213 °C; yield 2.0 g (70%). Elemental analysis calculated for $(Me_3C_{16}N)_2[CuBr_4]$, $C_{38}H_{84}N_2CuBr_4$ (952.26): C 47.60, H 8.84, N 2.88 (%), found: C 47.92, H 8.89, N 2.94 (%); IR (KBr, cm^{-1}): 2956m, 2925m $\nu_{symmetric}$ (sp^3 C–H), 2868m $\nu_{asymmetric}$ (sp^3 C–H), 1585m, 1484m, 1437s ν(C–C), 1112s ν(C–P), 995m, 900w, 748s, 725s γ(C–H), 691s ν(C–C).

Two weak bands appear in all UV-vis spectra of the bromidocuprate(II) complexes between 250 and 550 nm, which, according to the literature, are associated with ligand-to-metal charge transfer transitions,[70] since the d–d transitions of $[CuBr_4]^{2-}$ are expected in the near-IR region.[71] The broad bands around 550 nm are responsible for the colour of the complexes.

To obtain suitable single crystals for X-ray structure determination 1 mL of a concentrated solution of the tetrabromidocuprates in chloroform was covered with a layer of *n*-hexane and left undisturbed for some days to allow the interdiffusion of the solvents. After about two days, dark purple needles formed at the interface. The crystals were isolated and washed three times with diisopropyl ether.

Methods

Elemental analyses were carried out on an Elementar vario EL III analyzer. Infrared spectra were recorded on a Perkin–Elmer type 16PC FT-IR spectrophotometer between 4000 and 400 cm^{-1} as KBr-pellets (reference KBr). The melting points were determined with a 'Mikroheiztisch Boetius'.

EPR spectra were recorded at 9.4 GHz (X-band) with a Bruker CW Elexsys E 500 spectrometer and at ~34 GHz (Q-band) with a Bruker EMX spectrometer at 295 K. The spectra were simulated with the experimental parameters using Bruker Xsophe.[72]

Suitable crystals were mounted on a glass fibre. A crystal of **1** was embedded in perfluoroalkylether oil. X-Ray diffraction data were collected at 210 K on a STOE Imaging Plate Diffraction System IPDS-II using graphite monochromatized Mo-K_α radiation (λ = 0.71073 Å). The data were corrected by a spherical absorption correction using the program X-Area[73] as well as for Lorentz polarization and extinction effects. The solution of the crystal structure was performed using the program SHELXS-97 by direct methods,[74] and refined against F^2 by means of full-matrix least-squares procedures using the program SHELXL-97.[75] In the compounds **1–3**, all non-hydrogen atoms were refined anisotropically. In the case of **4**, only poor data sets could be obtained, in spite of attempts to collect diffraction data with several crystals. Therefore, the structure of **4** is essentially correct, but has only a limited accuracy. The disordered carbon atoms C55–C57 at N3 were refined isotropically. Besides both the peripheric carbon atoms (C15, C16) of one of the four alkyl-chains were disordered over two sites. In all structures the hydrogen atoms were calculated in their expected positions and refined with a riding model. For the visualisation of the structures the graphic program DIAMOND[76] was used. The crystallographic data as well as details of the refinement for the complexes $(BzlPh_3P)_2[CuBr_4]$ (**1**), $(MePh_3P)_2[CuBr_4]$ (**2**), $(Ph_4P)_2[CuBr_4]$ (**3**), and $(Me_3C_{16}N)_2[CuBr_4]$ (**4**) are listed in Table 1.

CCDC-818359 (**1**), CCDC-818358 (**2**), CCDC-818357 (**3**) and CCDC-818356 (**4**) contain the supplementary crystallographic data for this paper.

Density Functional Theory (DFT) calculations were done at the B3LYP/aug-cc-pVTZ level of theory for all calculations as implemented in the Gaussian09 program package.[77] The *g*-values were calculated using the Gauge-Independent Atomic Orbital (GIAO) method.[78]

Results

Single crystal X-ray structures of the complexes

Because the counter-cations contain no new information only the structural features of the tetrabromidocuprate dianions

View Article Online

Published on 05 October 2011. Downloaded by TU Berlin - Universitaetsbibl on 31/03/2016 12:42:47.

Table 1 Crystallographic data and refinement parameters for the tetrabromidocuprate(II) complexes **1–4**

Compound	$(BzlPh_3P)_2[CuBr_4]$ (**1**)	$(MePh_3P)_2[CuBr_4]$ (**2**)	$(Ph_4P)_2[CuBr_4]$ (**3**)	$(Me_3C_{16}N)_2[CuBr_4]$ (**4**)
Empirical formula	$C_{50}H_{44}P_2CuBr_4{\cdot}2CHCl_3$	$C_{38}H_{36}P_2CuBr_4$	$C_{48}H_{40}P_2CuBr_4$	$C_{38}H_{84}N_2CuBr_4$
M/g mol^{-1}	1328.71	937.79	1061.92	952.26
Crystal colour	Blue	Violet	Brown-violet	Violet
Crystal size/mm	0.55 × 0.38 × 0.30	0.95 × 0.46 × 0.16	1.10 × 0.41 × 0.05	1.2 × 0.2 × 0.05
Crystal form	Prism	Needle	Needle	Plate
Crystal system	Monoclinic	Monoclinic	Monoclinic	Triclinic
Space group	$P2_1/c$	Cc	$C2/c$	$P\bar{1}$
a/Å	18.6843(11)	8.9966(11)	10.8617(17)	9.3459(15)
b/Å	10.2238(6)	24.702(3)	19.554(2)	17.513(3)
c/Å	28.5236(15)	17.481(2)	21.072(3)	30.135(5)
α/°	90	90	90	77.197(14)
β/°	91.612(5)	101.553(10)	91.914(12)	86.123(14)
γ/°	90	90	90	84.763(13)
V/Å^3	5446.6(5)	3806.1(8)	4473.1(11)	4783.93(14)
Z	4	4	4	4
F(000)	2636	1852	2108	1980
Density/mg m^{-3}	1.620	1.637	1.577	1.322
μ/mm^{-1}	3.723	4.883	4.165	3.822
Θ range/°	1.43–25.0	2.03–25.00	1.93–25.00	1.20–24.84
R_{int}	0.0794	0.0851	0.0986	0.120
Refl. measured	34 342	12 264	14 297	29 666
Refl. independent	9574	6424	3952	15 318
Parameters	593	407	250	825
R_1/wR_2 [$I > 2\sigma(I)$]	0.0321/0.0662	0.0527/0.1301	0.0457/0.0869	0.0719/0.1516
R_1/wR_2 (all data)	0.0543/0.0717	0.0705/0.1408	0.0821/0.0961	0.2000/0.1930
Goodness of fit	0.910	0.993	0.910	0.833
Max. diff. peak/hole/e Å^3	−0.51/0.52	−0.81/0.86	−0.64/1.76	−0.929/0.790

and their crystal packing (Hydrogen contacts, Cu···Cu and B···Br distances) are discussed. For more structural details see ESI† (cif-files of the four structures). Table 1 summarizes the crystallographic data and refinement parameters for the tetrabromidocuprate(II) complexes **1–4**

Bis(benzyltriphenylphosphonium)tetrabromidocuprate(II) (1)

$(BzlPh_3P)_2[CuBr_4]{\cdot}2CHCl_3$ (**1**) crystallises in the non-centrosymmetric space group $P2_1/c$ with four formula units per unit cell. As shown in Fig. 1 the crystal structure of compound **1** is stabilised by hydrogen bonds between the bromine atoms of the bromidocuprate(II) and the chloroform hydrogen atom as well as between the bromine atom and the hydrogen atoms of the benzyl-CH_2 group. Less prominent hydrogen contacts are observed between the bromine atoms and the hydrogen atoms of the phenyl rings (see Table 2 and Fig. 1). The copper centres are well separated and due to the molecular packing the shortest Cu···Cu distances are 10.22 and 11.35 Å and the intermolecular Br···Br distances are in the range of 8.35 to 11.93 Å.

Bis(methyltriphenylphosphonium)tetrabromidocuprate(II) (2)

$(MePh_3P)_2[CuBr_4]$ (**2**) crystallises in the non-centrosymmetric space group Cc with four formula units per unit cell. The cations are composed of planar phenyl groups tetrahedrally arranged around the central phosphorus atoms and possess the usual standard bond lengths and angles. Table 3 lists the main bond lengths and angles. As expected the complex anion $[CuBr_4]^{2-}$ has a distorted tetrahedral geometry. The shortest Cu···Cu distances are 10.22 and 11.35 Å and the intermolecular Br···Br distances are between 9.00 and 10.98 Å, even if Fig. 2 suggests shorter contacts.

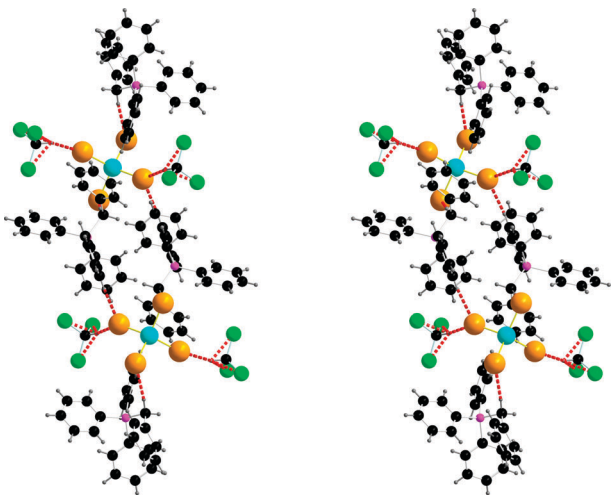

Fig. 1 Stereoscopic view on the crystal packing of $(BzlPh_3P)_2[CuBr_4]{\cdot}2CHCl_3$ (**1**).

The crystal structure of **2** is stabilised through several hydrogen bonds between the bromine atoms and the hydrogen atoms of the methyltriphenylphosphonium cations. The closest hydrogen contacts are listed in Table 3. From the crystal packing illustrated in Fig. 2 there is no indication of π–π-interactions between the phenyl rings of the cations.

Bis(tetraphenylphosphonium)tetrabromidocuprate(II) (3)

$(Ph_4P)_2[CuBr_4]$ **3** crystallises in the centrosymmetric space group $C2/c$ with four formula units per unit cell (Fig. 3). Similar to the previously discussed complexes the complex anion $[CuBr_4]^{2-}$ possesses a distorted tetrahedral geometry but with a 2-fold (C_2) rotational axis symmetry at the copper centre. The two cations

 This journal is © The Royal Society of Chemistry and the Centre National de la Recherche Scientifique 2011

View Article Online

Published on 05 October 2011. Downloaded by TU Berlin - Universitaetsbibl on 31/03/2016 12:42:47.

Table 2 Selected bond lengths and angles of $(BzlPh_3P)_2[CuBr_4]$ (**1**)

Bond lengths/Å		Angles/°	
Cu1–Br1	2.3904(5)	Br1–Cu1–Br2	128.25(2)
Cu1–Br2	2.3855(5)	Br1–Cu1–Br3	100.26(2)
Cu1–Br3	2.3860(5)	Br1–Cu1–Br4	99.86(2)
Cu1–Br4	2.3735(5)	Br2–Cu1–Br3	100.76(2)
		Br2–Cu1–Br4	100.56(2)
		Br3–Cu1–Br4	131.31(2)

Hydrogen contacts	C···Br	Sym.
C1–H1B···Br3	3.727(4)	2655
C26–H26A···Br4	3.693(4)	2655
C35–H35···Br4	3.748(4)	2645
C37–H37···Br1	3.711(4)	4664
C51–H51···Br2	3.679(5)	1565
C52–H52···Br1	3.609(5)	4564

Symmetry transformation used to generate equivalent atoms

1565 = x, 1 + y, z
2645 = 1 − x, −1/2 + y, 1/2 − z
4664 = 1 + x, 3/2 − y, − 1/2 + z
4564 = x, 3/2 − y, −1/2 + z

Table 3 Selected bond lengths and angles of $(MePh_3P)_2[CuBr_4]$ (**2**)

Bond lengths/Å		Angles/°	
Cu1–Br1	2.394(1)	Br1–Cu1–Br2	97.12(5)
Cu1–Br2	2.359(1)	Br1–Cu1–Br3	139.71(6)
Cu1–Br3	2.389(2)	Br1–Cu1–Br4	99.00(5)
Cu1–Br4	2.364(2)	Br2–Cu1–Br3	94.91(6)
		Br2–Cu1–Br4	137.59(6)
		Br3–Cu1–Br4	97.51(7)

Closest hydrogen contacts	C···Br	Sym
C8–H8···Br1	3.677(9)	
C12–H12···Br1	3.683(9)	4454
C15–H15···Br4	3.646(13)	4354
C19–H19C···Br2	3.771(14)	
C21–H21···Br3	3.611(9)	
C27–H27···Br2	3.447(9)	2655
C31–H31···Br1	3.779(12)	1655
C38–H38C···Br3	3.858(13)	

Symmetry transformation used to generate equivalent atoms

4454 = −1/2 + x, 1/2 − y, −1/2 + z
4354 = −3/2 + x, 1/2 − y, −1/2 + z
2655 = 1 + x, −y, 1/2 + z
1655 = 1 + x, y, z

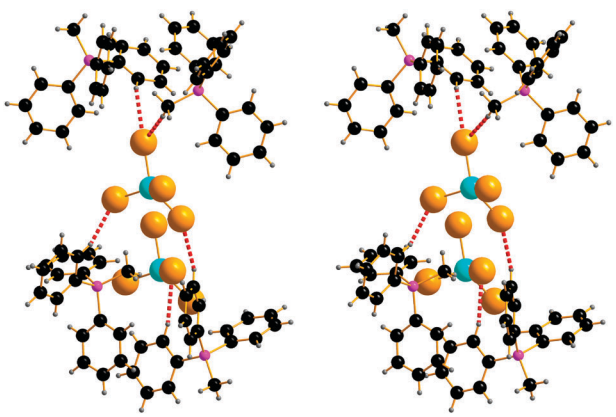

Fig. 2 The molecular structure of $(MePh_3P)_2[CuBr_4]$ (**2**).

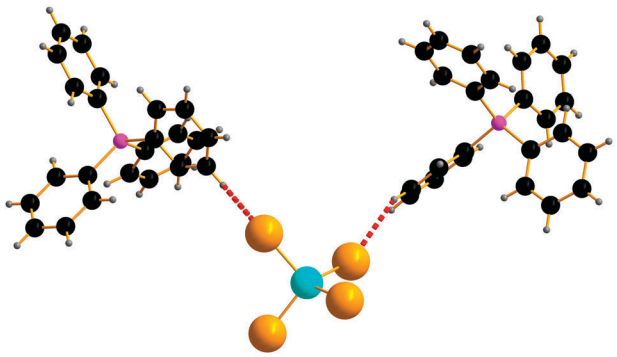

Fig. 3 The molecular structure of $(Ph_4P)_2[CuBr_4]$ (**3**).

Table 4 Selected bond lengths and angles of $(Ph_4P)_2[CuBr_4]$ (**3**)

		Bond lengths/Å	Angles/°
Cu1–Br1	2.394(1)	Br1–Cu1–Br1^{i}	105.07(5)
Cu1–Br2	2.359(1)	Br1–Cu1–Br2	100.41(2)
		Br1–Cu1–Br2^{i}	124.19(2)
		Br2–Cu1–Br2^{i}	102.71(2)

Closest hydrogen contacts		C···Br	Sym.
C5–H5···Br2		3.674	8445

Symmetry transformation used to generate equivalent atoms

(i)	−x, y, 1.5 − z;	8445	x − 0.5, −y − 0.5, 0.5 + z

do not exhibit structural characteristics and are, therefore, not discussed further. The corresponding main bond lengths and angles are listed in Table 4.

In contrast to the complex $(MePh_3P)_2[CuBr_4]$ **2** the crystal structure of $(Ph_4P)_2[CuBr_4]$ **3** is stabilised through just one hydrogen bond between the bromine atom Br2 and the hydrogen atom H21 of the aromatic ring of the cation. This could be one of the reasons for the less pronounced deviation from a perfectly tetrahedral structure in the $[CuBr_4]^{2-}$ moiety (Br–Cu–Br = 109.5°). The copper centres in **3** are also relatively well separated. The shortest Cu···Cu distances are 10.67, 10.86 and 11.18 Å and the intermolecular Br···Br distances are between 7.76 and 11.69 Å. Selected structural data, bond angles and distances are given in Table 4.

Bis(hexadecyltrimethylammonium)tetrabromidocuprate(II) (4)

$(Me_3C_{16}N)_2[CuBr_4]$ **4** crystallises in the centrosymmetric space group $P\bar{1}$ with four formula units per unit cell, two per asymmetric unit. Hydrogen-bonding interactions between the bromine atoms and the hydrogen atoms of the cations are not recognised. Fig. 4 shows a section of the crystal structure with discrete anions and cations arranged in lamellar fashion with alternating hydrophobic and hydrophilic regions, which often supports the effective packing and thus the crystallisation process. The alkyl chains of the cations are all in *trans* conformation. Some carbon atoms of the cations are slightly disordered. Each copper centre is a distorted tetrahedron surrounded by four bromide ions. The corresponding bond lengths and angles are given in Table 5. The copper centres in **4** have the shortest contacts of the complexes studied here. Due to the lamellar packing the shortest Cu···Cu distances are

View Article Online

Published on 05 October 2011. Downloaded by TU Berlin - Universitaetsbibl on 31/03/2016 12:42:47.

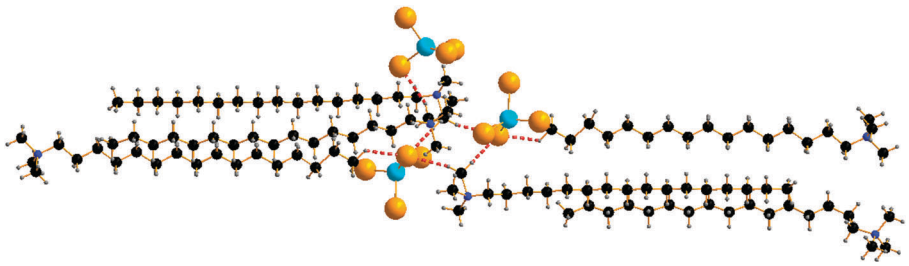

Fig. 4 Part of the crystal packing of $(Me_3C_{16}N)_2[CuBr_4]$ (**4**).

Table 5 Selected bond lengths and angles of $(Me_3C_{16}N)_2[CuBr_4]$ (**4**)

Bond lengths/Å		Angles/°	
Cu1–Br1	2.404(2)	Br1–Cu1–Br2	100.05(7)
Cu1–Br2	2.356(2)	Br1–Cu1–Br3	97.66(8)
Cu1–Br3	2.412(2)	Br1–Cu1–Br4	133.51(9)
Cu1–Br4	2.353(2)	Br2–Cu1–Br3	132.22(9)
		Br2–Cu1–Br4	100.17(8)
		Br3–Cu1–Br4	98.88(9)
Cu2–Br5	2.363(2)	Br5–Cu2–Br6	102.71(7)
Cu2–Br6	2.405(2)	Br5–Cu2–Br7	133.72(8)
Cu2–Br7	2.365(2)	Br5–Cu2–Br8	98.70(7)
Cu2–Br8	2.407(2)	Br6–Cu2–Br7	99.21(7)
		Br6–Cu2–Br8	124.70(7)
		Br7–Cu2–Br8	101.43(7)

Closest hydrogen contacts	C···Br	Sym.
C38–H38B···Br8	3.845(15)	1655
C38–H38C···Br4	3.754(16)	1655
C55A–H55F···Br8	3.76(3)	
C55A–H56E···Br7	3.58(3)	
C161–H161···Br7	3.57(4)	2875

Symmetry transformation used to generate equivalent atoms

1655 = 1 + x, y, z	2875 = 3 − x, 2 − y, −z

between 8.07 and 9.41 Å and the shortest intermolecular Br···Br distances are rather small at 4.71 Å.

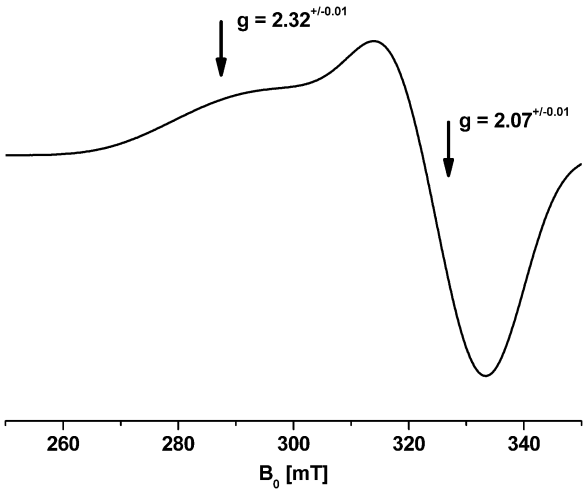

Fig. 5 X-Band powder EPR spectrum of $(BzlPh_3P)_2[CuBr_4]$ (**1**).

Table 6 Experimental EPR parameters ($g_{||}$- and $g_{\perp}$-values)

Compound	$g_{\|\|}$	$g_{\perp}$	g_{av}
$(BzlPh_3P)_2[CuBr_4]$ (**1**)	2.32 ± 0.01	2.07 ± 0.01	2.153 ± 0.005
$(MePh_3P)_2[CuBr_4]$ (**2**)	2.30 ± 0.01	2.07 ± 0.01	2.147 ± 0.005
$(Ph_4P)_2[CuBr_4]$ (**3**)	2.29 ± 0.01	2.07 ± 0.01	2.143 ± 0.005
$(Me_3C_{16}N)_2[CuBr_4]$ (**4**)	2.22 ± 0.01	2.08 ± 0.01	2.127 ± 0.005

EPR-spectroscopy

To prevent or minimize magnetic interactions between the Cu(II) centres (which broaden the lines in the EPR spectra) a diamagnetic dilution is necessary. This can be achieved by a solvent or by doping into a diamagnetic host lattice. In both cases the structure of the tetrabromidocuprate dianion is affected, which is not desirable, if structural aspects are investigated. Instead, we therefore used sterically rather demanding cations, which should result in sufficient diamagnetic dilution by separating the paramagnetic bromidocuprate(II) moieties from one another.

Despite this approach, however, the EPR line broadening results in a missing hyperfine structure for the copper(II) ion for both Cu isotopes (^{63}Cu, ^{65}Cu; nuclear spin $I = 3/2$ each) and the four bromide ligands (^{79}Br, ^{81}Br; nuclear spin $I = 3/2$ each). The experimental spectrum of **1** (Fig. 5) shows that the hyperfine structure in X-band EPR is not resolved at all. This is mainly caused by the exchange broadening due to the still incomplete separation of the paramagnetic centres. The distances between the paramagnetic centres in the complexes **1–4** are in the range of 8 to 10.9 Å. All EPR spectra measured at 9.5 GHz (X-band) seem to correspond to an axial g-tensor showing broad signals. No coupling parameters can be extracted. For a better resolution these complexes were also measured at ~34 GHz (Q-band).

Q-band spectra are better resolved and the basic parameters $g_{||}$ and $g_{\perp}$ could be determined. The spectra indicate an axially symmetric species, which is consistent with the compressed tetrahedral stereochemistry of the $[CuBr_4]^{2-}$ chromophore determined from the crystal structure and the relation $g_{||} \gg g_{\perp} > 2.0$ indicates a $b_1(d_{x^2-y^2})$ ground state.[79] The principle values of the electron Zeemann tensor, the $g_{||}$- and $g_{\perp}$-values, of the complexes are collected in Table 6 and two of the corresponding EPR spectra are shown in Fig. 6.

Quantum chemical calculations

Tetrahedral/planar distortions in copper complexes were already investigated using the Continuous Symmetry Measure (CSM) methodology (see *e.g.* ref. 80–82). In CSM all structural parameters are incorporated in the analysis. As already stated, in this work, we try to correlate structural and EPR-parameters for applications in solution, especially in ionic liquids, where

 This journal is © The Royal Society of Chemistry and the Centre National de la Recherche Scientifique 2011

View Article Online

Published on 05 October 2011. Downloaded by TU Berlin - Universitaetsbibl on 31/03/2016 12:42:47.

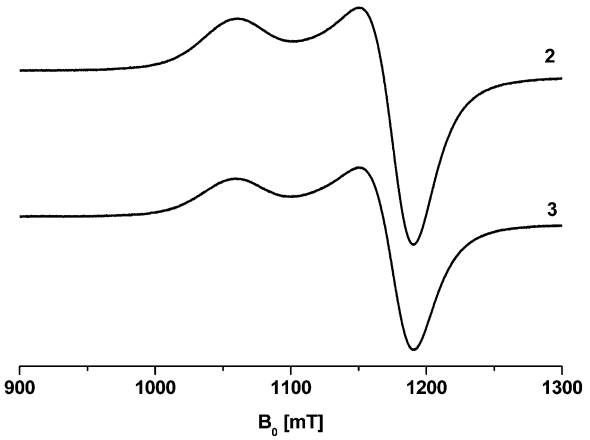

Fig. 6 Q-Band EPR powder spectra of the complexes **2** and **3**.

precise structural parameters are often unknown. Therefore, we resort to a simpler model, which describes the distortion by a single parameter, *i.e.*, the *cis*-angle. Here, we choose structures along the spread mode (see below), which was found to be the minimum energy path in theoretical calculations for $[CuCl_4]^{2-}$ and very close to most experimental structures for d^9 ions in the CSM studies.

The basic model is sketched in Fig. 7. In order to create different *cis*-angles along the spread mode the bond angles Φ between Br(a)–Cu–Br(a') and Br(b)–Cu–Br(b') are varied simultaneously starting from the square planar configuration ($\Phi = 180°$). For $\Phi < 180°$ Br(a) and Br(a') are displaced "above" the paper plane and Br(b) and Br(b') "below". By this choice, we obtain D_{4h} symmetry for $\Phi = 180°$, D_{2d} for $180° > \Phi > 109.471°$ and T_d for $\Phi = 109.47°$. Due to the symmetry all four Cu–Br bond distances r are identical and also all *cis*-angles. The *cis*-angles for $\Phi = 180°$, 150°, 140°, 130°, 120°, and 109.471° are 90°, 93.8°, 96.7°, 100.3°, 104.5°, and 109.471°, respectively. For all *cis*-angles the bond distances r were optimised. We also performed an optimisation for Φ and r.

We did the calculation for the gas phase and using a polarizable continuum model (PCM) approach[83] for acetonitrile ($\varepsilon = 35.688$) and water ($\varepsilon = 78.355$). Frequency calculations confirmed that the optimised D_2h conformers for different environments are indeed minima on the potential energy surface. Furthermore, test calculations for the gas phase case using different initial bond lengths r for the optimisation of the intermediate structures resulted (within numerical accuracy) in a single value for all four Cu–Br bond lengths in the complex, indicating that the spread path is also the minimum energy path in the present case.

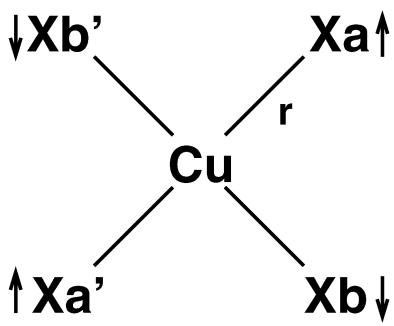

Fig. 7 Sketch of the model.

For the gas phase calculations we obtain positive energies for some occupied Kohn–Sham orbitals, while for the PCM calculations all orbitals have negative energies. All calculations have been done for a spin multiplicity 2 and the total charge −2. The optimised *cis*-angles are 100.8° in the gas phase, 100.1° in acetonitrile and 100.2° in water. The electronic energy relative to the optimised geometry as a function of the *cis*-angle is nearly independent of the environment. Also the bond distances, r, are rather constant for different angles and environments. However, r is a little too long compared to experimental structure data, probably due to the two uncompensated negative charges in the system. A clear trend for the Mulliken charge at the Cu atom as a function of the *cis*-angle can be seen, at least for the gas phase calculations. However, this trend is much more pronounced for the Mulliken spin density at the Cu atom and nearly independent of the environment (see Fig. 8).

In Fig. 9 the spin density distribution in the $[CuBr_4]^{2-}$ *versus* the variation of the coordination geometry is visualised. The unpaired electron is mainly localized at the copper centre. The different geometries generate a change in the overlap of the involved atomic orbitals (angular overlap) and, therefore, a modification of the spin situation with increasing spin density at the Cu(II) from square planar towards tetrahedral coordination. This is also reflected in the EPR parameters, showing an increasing g value due to the increasing spin density at the Cu(II) centre (see Fig. 10).

Discussion

The stereochemistry of the halidocuprate ion is intensely studied because of its enormous structural variety. This variety is related to its structural flexibility as well as its ability to form

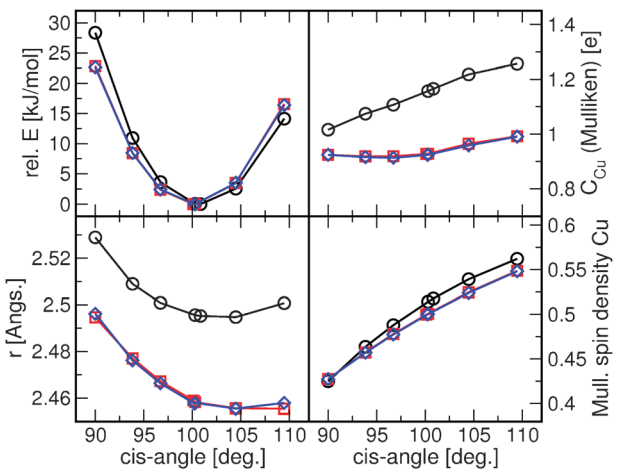

Fig. 8 Electronic energy relative to the optimised structure, Cu–Br distance r and the Mulliken charge of the Cu atom depending on the *cis*-angle for different environments (gas phase, acetonitrile, water). Mulliken spin density at the Cu atom depending on the *cis*-angle for different environments (gas phase ○, acetonitrile □, water ◊). The values for acetonitrile and water are essentially overlapping.

View Article Online

Published on 05 October 2011. Downloaded by TU Berlin - Universitaetsbibl on 31/03/2016 12:42:47.

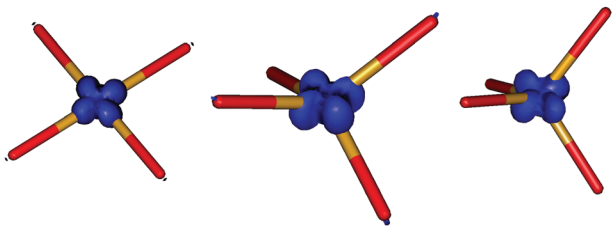

Fig. 9 Correlation of the averaged *cis*-angles to the averaged *g*-values for tetrabromidocuprate(II) complexes (square planar 90°, perfect tetrahedron 109.5°). The straight line reflects the linear fit of the experimental data and the dotted line the calculated *g*-values from the DFT calculations. The numbering scheme is according to Table 7, the diamond labels (on dotted line) are according to the DFT calculations.

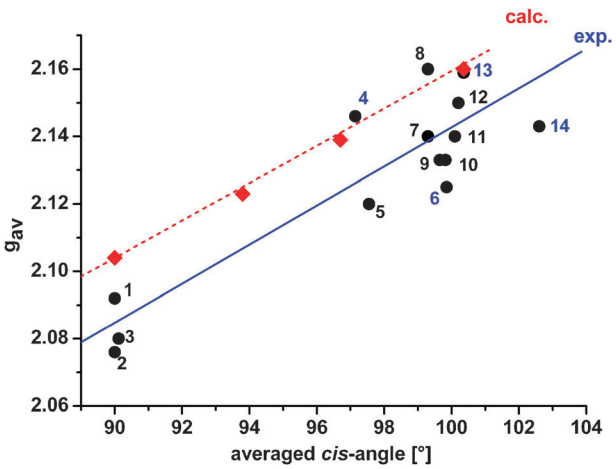

Fig. 10 Spin density distribution in $[CuBr_4]^{2-}$ in the square planar geometry (left), the optimised structure (middle) and the tetrahedral geometry (right). The spin densities are obtained from the acetonitrile PCM approach.

many structural types varying from monomers, dimers, and oligomers up to cluster structures.[84,85] Sometimes different structures are present in the same solution. In the case of tetrahalidocuprates(II) the structure of the $[MX_4]^{2-}$ moiety varies from distorted tetrahedral to square planar. This variation is not arbitrary; there are factors influencing the degree of distortion, which can be grouped into five categories using simple electrostatic arguments:

A: *Jahn–Teller effect*: The Jahn–Teller theorem does not provide information about favoured geometries. It states however which geometries should not be stable. For the d^9 Cu(II) system, this precludes the perfect tetrahedral geometry. Indeed there are no known Cu(II) complexes with an exact tetrahedral geometry. All non-planar complexes show a distorted tetrahedral geometry, "compressed tetrahedron" and D_{2h} symmetry or even lower.[52,86]

B: *Crystal field stabilisation*: The largest stabilisation occurs for the geometry which gives the strongest bonds. Therefore the crystal field stabilisation factor supports the formation of almost square planar geometries, in which halide–copper bonds are stronger than those bonds in the tetrahedral geometry.[86]

C: *Ligand–ligand repulsion*: The electrostatic repulsion between the halide ions plays an important role in determining the coordination geometry since it strongly favours tetrahedral geometry. Since the Br atom is larger than the Cl atom, the distortion towards a tetrahedral geometry would weaken ligand–ligand repulsions.[14]

D: *Ligand–lattice interactions*: Interactions including (1) simple electrostatic interactions between the halide ions and the counter ions, (2) bonding interactions with neighbouring Cu(II) ions (as an evidence for the formation of Cu–X–Cu bridges), and (3) hydrogen bonding between the halide ions either with the counter ions or the lattice solvent molecules all reduce the effective charge on the halide ions. This in turn reduces the ligand–ligand repulsion effects. The role of the hydrogen bonding in stabilising the square-planar configuration through the removal of charge from the halide ion has been used in the interpretation of the coordination geometry of tetrahalidocuprates(II).[14,27,50,60,64,87,88] Generally, with weak hydrogen bonding electrostatic forces dominate and yield a geometry close to tetrahedral. With strong hydrogen bonding the crystal field stabilisation energy dominates, which yields a geometry closer to square planar.

E: *Crystal packing effects*: This category takes into account all effects that are not contained in the previous categories. Essentially, crystal packing effects are important because the shape and size of the counter ions may force the lattice into some particular form. The copper(II) halide species may then have to adjust its stereochemistry to best be accommodated into the packing arrangement.[89] Crystal packing effects include π–π interactions, which further stabilise the solid-state structures[90] and consequently also the symmetric or asymmetric geometry of the counter ions, shape and length of alkyl chains contained in the counter ions.

EPR spectroscopy is a powerful tool to characterize the coordination geometry of copper(II).[91–94] Already in 1980 A. Bencini, D. Gatteschi and C. Zanchini discussed the EPR spectra of the copper(II) doped complex dichloridobis-(triphenylphosphineoxide)zinc(II) with a distorted tetrahedral coordination geometry as single crystals and polycrystalline powders. These experiments were further supported by quantum chemical calculations comparing the spin Hamiltonian parameters CuX_2Cl_2 chromophores (X = Cl, N, O), reflecting a high covalency and large spin–orbit coupling of the Cu–Cl bonds.[95] A more recent theoretical study of $[MX_4]^{2-}$ (X = Cl, Br) by V. I. Murav'ev[96] provides a detailed discussion of the electronic situation in tetrahalidocuprates for square planar coordination, which is in good agreement with the experimental parameters.[97] M. T. Kite and J. E. Drumheller[98] discussed in 1983 the *g*-values for a series of tetrachlorido- and tetrabromidocuprate(II) salts combined with a line width analysis showing that the bromide complexes have significantly lower *g*-values than the analogous chloride complexes with identical cations. This is due to the stronger spin–orbit coupling in bromide salts as also confirmed by R. D. Willett *et al.* since ligand spin–orbit coupling reduces the *g*-values.[99–101] A. Bencini and D. Gatteschi calculated the electronic and EPR parameters of $[MCl_4]^{2-}$ on the SCF-MS-X_α-level for square planar and "pseudotetrahedral" coordination geometries.[102] In agreement with experimental data larger

 This journal is © The Royal Society of Chemistry and the Centre National de la Recherche Scientifique 2011

View Article Online

Published on 05 October 2011. Downloaded by TU Berlin - Universitaetsbibl on 31/03/2016 12:42:47.

g-values were found for the "pseudotetrahedral" geometry compared to a square planar coordination.

S.-K. Kang *et al.*[51] attempted a correlation of the EPR-parameters (g_{av}) with the degree of distortion (θ, *i.e.* the average of the largest two angles, the *trans*-angles) of tetrachloridocuprate(II) complexes. The EPR spectra in their study were recorded in frozen glass ($DMF:CH_2Cl_2 = 1:1$), where the structural situation may be significantly different than in the neat compounds, due to the interaction with the solvent and possibly affected by the freezing process. In spite of this, the study shows that the larger the *trans*-angle, the smaller is the experimental *g*-value. Here we correlate the experimental EPR data in the pure solid substances (not in a glass or liquid) with the structural parameters of our tetrabromidocuprate(II) complexes **1–4** and complexes, whose crystal structure and EPR parameters are reported in the literature. In contrast to the study mentioned above,[51] we do not use the *trans*-angle, but the averaged *cis*-angle (*i.e.* the average of the smallest four Br–Cu–Br angles) because of the particularly strong distortion. The average *g*-values (g_{av}) were obtained through the following relation between the anisotropic parameters of the *g*-tensor, eqn (1):

$$g_{av} = \frac{g_{\parallel} + 2 \cdot g_{\perp}}{3} \quad (1)$$

Table 7 summarizes the data extracted from the literature and the additional data obtained from our new complexes. Fig. 10 reveals a direct relation between the averaged *cis*-angles and the corresponding g_{av}-values ($R = 0.8259$), taking into account that the averaged *g*-values g_{av} increase as the geometry of the structure of $[CuBr_4]^{2-}$ anions changes from square planar to distorted tetrahedral. The complexes with a square planar coordination geometry (*cis*-angle 90°) $[CuBr_4]^{2-}$ have g_{av}-values < 2.10. Beginning at a *g*-value of about 2.12 the $[CuBr_4]^{2-}$ anions show a tendency towards more or less distorted or compressed tetrahedral geometries. This trend of increasing *g*-values with increasing *cis*-angles is in good agreement with the calculated Mulliken spin density at the copper centre (Fig. 8) and the trend of *g*-values calculated *via* DFT (dotted line in Fig. 10). It must be noted however, that, while the trend is the same, the absolute values obtained from DFT are about 0.02 higher than the values obtained from a linear regression analysis of the experimental data.

Table 7 Averaged *cis*-angles and averaged *g*-values of available tetrabromidocuprate(II) complexes

Entry	Formula	*cis*-Angle/°	g_{av}	Ref.
1	$K_2[Pd(Cu)Br_4]$	90.00	2.092	58
2	$(NH_4)_2[CuBr_4]$	90.00	2.076	59
3	$(\beta\text{-alaH})_2[CuBr_4]$	90.12	2.080	101
4	$(MePh_3P)_2[CuBr_4]$	97.14	2.146	This work (**2**)
5	$(4\text{-Et-Py})_2[CuBr_4]$	97.55	2.120	61
6	$(Me_3C_{16}N)_2[CuBr_4]$	99.85	2.125	This work (**4**)
7	$(2\text{-apyH})_2[CuBr_4]$	99.30	2.140	62
8	$(4\text{-apyH})_2[CuBr_4]$	99.30	2.16	63
9	$(Ph_3AsOH)_2[CuBr_4]$	99.65	2.133	10
10	$(pipdH)_2[CuBr_4]$	99.825	2.133	65
11	$(3\text{-Et-Py})_2[CuBr_4]$	100.10	2.140	61
12	$(4\text{-Me-Py})_2[CuBr_4$	100.20	2.15	60
13	$(BzlPh_3P)_2[CuBr_4]$	100.36	2.159	This work (**1**)
14	$(Ph_4P)_2[CuBr_4]$	102.65	2.148	This work (**3**)

We would like to stress once more that the aim of this study was not to achieve best resolution or the use of highly sophisticated EPR techniques but to provide a tool to obtain structure information of tetrabromidocuprates $[CuBr_4]^{2-}$ in non-crystalline samples (*e.g.* ionic liquids, liquid crystals or solution) by cw-X-band EPR spectroscopy. For average *cis*-angles with values between 91° and 97° unfortunately no complete data (X-ray and EPR) are available in the literature. More work is therefore required to fill this gap and to further refine the correlation.

Conclusion

The aim of this work was the synthesis of a series of new tetrabromidocuprate(II) complexes and the correlation of their structures, in particular the geometry of the $[CuBr_4]^{2-}$ obtained from X-ray crystallography with the g_{av}-value obtained from EPR measurements of the solid and pure (*i.e.* undissolved) complexes. To sufficiently separate the paramagnetic centres from each other sterically quite demanding cations were used. The EPR spectra in the X-band were only very poorly resolved (no hyperfine structure), which can be assigned to exchange broadening caused by incomplete separation of the paramagnetic centres. The Q-band EPR spectra allowed for the determination of the *g*-tensor parameters. The complexes with the cations: benzyltriphenylphosphonium, methyltriphenylphosphonium, tetraphenylphosphonium, and hexadecyltrimethylammonium crystallised as monomeric complexes and the X-ray structures show that the tetrabromidocuprate(II) anions present in all cases a compressed tetrahedral geometry with two types of bond angles distinguishing their "*trans*" values (124°–140°) from the "*cis*" angles (94°–106°). These values show that the coordination geometry of most tetrabromidocuprates is an intermediate between square planar (D_{4h}) and regular tetrahedral (T_d). This is in good agreement with the results from DFT calculations. The electrostatic repulsion forces between the bromide ions seem to dominate, which yields structures close to a more tetrahedral geometry with mean *cis*-angles of 102.65° and 99.14°, respectively.

The key finding of this work is that there is a correlation between the tetrabromidocuprate geometry and the average *g*-value g_{av}. Tetrabromidocuprates(II) with a geometry close to square planar possess average *g*-values less than ~2.12. With increasing distortion towards tetrahedral geometry the average *g*-values raise accordingly. This correlation is applicable for the structural characterisation of tetrabromidocuprate(II) complexes in general and those which are ionic liquids in particular, *e.g.* to gain structure information when metal containing ionic liquids are used as precursors for CuCl materials.[103] Part 2 of this study will deal with the related tetrachloridocuprates(II) and some applications.

Acknowledgements

Financial support by the Ministry of Higher Education of Syria (R. F.), German Research Council, the University of

View Article Online

Published on 05 October 2011. Downloaded by TU Berlin - Universitaetsbibl on 31/03/2016 12:42:47.

Potsdam, the MPI of Colloids and Interfaces (Colloid Chemistry Department) is gratefully acknowledged.

References

1 L. Helmholz and R. F. Kruh, *J. Am. Chem. Soc.*, 1952, **74**, 1176.
2 N. S. Gill and R. S. Nyholm, *J. Chem. Soc.*, 1959, 3997.
3 G. Felsenfeld, *Proc. R. Soc. London, Ser. A*, 1956, **236**, 506.
4 D. M. Gruen and C. A. Angel, *Inorg. Nucl. Chem. Lett.*, 1966, **2**, 75.
5 P. S. Gentile, T. A. Shankoff and J. Carlotto, *J. Inorg. Nucl. Chem.*, 1967, **29**, 1393.
6 H. T. Witteveen, D. L. Jongejan and W. Brandwijk, *Mater. Res. Bull.*, 1974, **9**, 345.
7 E. R. Jones, M. E. Hendricks, S. L. Finkiea, L. Cathey, T. Auel and E. L. Emma, *J. Chem. Phys.*, 1970, **52**, 1922.
8 R. Puget, M. Jannin, R. Perret, L. Godefroy and G. Godefroy, *Ferroelectrics*, 1990, **107**, 229.
9 H. Suzuki and T. Watanabe, *Phys. Lett. A*, 1967, **26**, 103.
10 A. C. Massabni, O. R. Nascimento, K. Halvorson and R. D. Willett, *Inorg. Chem.*, 1992, **31**, 1779.
11 R. Willett, H. Place and M. Middleton, *J. Am. Chem. Soc.*, 1988, **110**, 8639.
12 A. Tosik and M. Bukowska-Strzyzewska, *J. Crystallogr. Spectrosc. Res.*, 1989, **19**, 707.
13 R. Bhattacharya, S. Chanda, G. Bocelli, A. Cantoni and A. Ghosh, *J. Chem. Crystallogr.*, 2004, **43**, 393.
14 H. Place and R. D. Willett, *Acta Crystallogr., Sect. C: Cryst. Struct. Commun.*, 1988, **44**, 34.
15 R. D. Willett, J. A. Haugen, J. Lebsack and J. Morrey, *Inorg. Chem.*, 1974, **13**, 2510.
16 M. Natarajan and E. A. Secco, *Phys. Status Solidi A*, 1976, **88**, 427.
17 G. Amirthaganesan, M. A. Kandhaswamy and V. Srinivasan, *Cryst. Res. Technol.*, 2006, **41**, 1096.
18 S. A. Roberts, D. R. Bloomquist, R. D. Willett and H. W. Dodgen, *J. Am. Chem. Soc.*, 1981, **103**, 2603.
19 J. D. Woodward, J. Choi and J. L. Musfeldt, *Phys. Rev. B: Condens. Matter Mater. Phys.*, 2005, **71**, 1.
20 M. M. Turnbull, C. P. Landee and B. M. Wells, *Coord. Chem. Rev.*, 2005, **249**, 2567.
21 R. D. Willett, D. Gatteschi, and O. Kahn, *Magneto-Structural Correlations in Exchange Coupled Systems*, Reidel, Boston, 1985, 389.
22 C. P. Landee, M. M. Turnbull, C. Galeriu, J. Giantsidis and F. M. Woodward, *Phys. Rev. B: Condens. Matter*, 2001, **63**, 100402.
23 R. T. Butcher, M. M. Turnbull, C. P. Landee, A. Shapiro, F. Xiao, D. Garrett, W. T. Robinson and B. Twamley, *Inorg. Chem.*, 2010, **49**, 427.
24 J. L. Wikaira, L. Li, R. Butcher, C. M. Fitchett, G. B. Jameson, C. P. Landee, S. G. Telfer and M. M. Turnbull, *J. Coord. Chem.*, 2010, **63**, 2949.
25 M. Deumal, G. Giorgi, M. A. Robb, M. M. Turnbull, C. P. Landee and J. J. Novoa, *Eur. J. Inorg. Chem.*, 2005, 4697.
26 A. Shapiro, C. P. Landee, M. M. Turnbull, J. Jornet, M. Deumal, J. J. Novoa, M. A. Robb and W. Lewis, *J. Am. Chem. Soc.*, 2007, **129**, 952.
27 H. Place and R. D. Willett, *Acta Crystallogr., Sect. C: Cryst. Struct. Commun.*, 1987, **43**, 1497.
28 K. Sperling, S. Linhard, W. Trautmann and H. Smuda, *EP* 0 325 784 A2, 1989.
29 C. J. Bowlas, D. W. Bruce and K. R. Seddon, *Chem. Commun.*, 1996, 1625.
30 F. Neve, O. Francescangeli, A. Crispini and J. Charmant, *Chem. Mater.*, 2001, **13**, 2032.
31 F. Neve, O. Francescangeli and A. Crispini, *Inorg. Chim. Acta*, 2002, **338**, 51.
32 F. Neve and A. Crispini, *Cryst. Growth Des.*, 2001, **1**, 387.
33 F. Neve and A. Crispini, *Cryst. Growth Des.*, 2001, **1**, 519.
34 A. Taubert, *Angew. Chem., Int. Ed.*, 2004, **43**, 5380.
35 A. Taubert, C. Palivan, O. Casse, F. Gozzo and B. Schmitt, *J. Phys. Chem. C*, 2007, **111**, 4077.
36 A. Taubert, P. Steiner and A. Mantion, *J. Phys. Chem. B*, 2005, **109**, 15542.
37 F. Neve, A. Crispini and S. Armentano, *Chem. Mater.*, 1998, **10**, 1904.
38 F. Neve and O. Francescangeli, *Cryst. Growth Des.*, 2005, **5**, 163.
39 F. Neve and A. Crispini, *CrystEngComm*, 2007, **9**, 698.
40 F. Neve and A. Crispini, *CrystEngComm*, 2003, **5**, 265.
41 F. Neve, A. Crispini and O. Francescangeli, *Inorg. Chem.*, 2000, **39**, 1187.
42 K. Binnemans, *Chem. Rev.*, 2005, **105**, 4148.
43 K. Goossens, K. Lava, P. Nockemann, K. van Hecke, L. van Meervelt, K. Driesen, C. Görller-Walrand, K. Binnemans and C. Cardinaels, *Chem.–Eur. J.*, 2009, **15**, 656.
44 F. J. Martinez Casado, M. Ramos Riesco, I. da Silva, A. Labrador, M. I. Redondo, M. V. Garcia Perez, S. Lopez-Andres and J. A. Rodriguez Cheda, *J. Phys. Chem. B*, 2010, **114**, 10075.
45 J.-M. Suisse, L. Douce, S. Bellemin-Laponnaz, A. Maisse-Francois, R. Welter, Y. Miyake and Y. Shimizu, *Eur. J. Inorg. Chem.*, 2007, 3899.
46 W. Dobbs, J.-M. Suisse, L. Douce and R. Welter, *Angew. Chem., Int. Ed.*, 2006, **45**, 4179.
47 C. K. Lee, H. H. Peng and I. J. B. Lin, *Chem. Mater.*, 2004, **16**, 530.
48 R. Hoffmann, *Am. Sci.*, 1997, **86**, 15.
49 O. V. Koval'Chukova, S. B. Strashnova, A. I. Stash, V. K. Bel'skii and B. E. Zaitsev, *Russ. J. Coord. Chem.*, 2009, **35**, 496.
50 R. L. Harlow, W. J. Wells, G. W. Watt and S. H. Simonsen, *Inorg. Chem.*, 1975, **14**, 1768.
51 S.-K. Kang, H.-S. Kim and Y.-I. Kim, *Bull. Korean Chem. Soc.*, 2006, **27**, 1877.
52 B. Murphy and B. Hathaway, *Coord. Chem. Rev.*, 2003, **243**, 237.
53 M. Acatellom, A. Girolamo and V. Usico, *J. Chem. Soc., Faraday Trans. 1*, 1981, **77**, 2367.
54 R. D. Willett and M. Extine, *Phys. Lett.*, 1973, **23**, 281.
55 R. A. Vaughan, *Phys. Status Solidi B*, 1972, **49**, 247.
56 T. Sato and T. Nakamura, *J. Chem. Technol. Biotechnol.*, 1984, **34A**, 375.
57 R. H. Borcherts, *Phys. Rev. B: Solid State*, 1970, **2**, 23.
58 C. Chow, K. Chang and R. D. Willett, *J. Chem. Phys.*, 1973, **59**, 2629.
59 E. Di Mauro and S. M. Domiciano, *Phys. B*, 2001, **304**, 398.
60 A. Luque, J. Sertucha, O. Castillo and P. Roman, *New J. Chem.*, 2001, **25**, 1208.
61 A. Luque, J. Sertucha, O. Castillo and P. Roman, *Polyhedron*, 2002, **21**, 19.
62 A. Luque, J. Sertucha, L. Lezama, T. Rojo and P. Román, *J. Chem. Soc., Dalton Trans.*, 1997, 847.
63 P. Roman, J. Sertucha, A. Luque, L. Lezama and T. Rojo, *Polyhedron*, 1996, **15**, 1253.
64 G. S. Long, M. Wei and R. D. Willett, *Inorg. Chem.*, 1997, **36**, 3102.
65 B. R. Patyal, B. L. Scott and R. D. Willett, *Phys. Rev. B: Condens. Matter*, 1990, **41**, 1657.
66 A. Taubert, *Top. Curr. Chem.*, 2009, **290**, 127.
67 C. Furlani and G. Morpurgo, *Theor. Chim. Acta*, 1963, **1**, 102.
68 H. Liu, X. Wang, W. Hu, L. Guo and S. Ouyang, *Chem. J. Internet*, 2004, **6**, 39, 066039ne.
69 M. M. El Essawi, *Transition Met. Chem.*, 1997, **22**, 117.
70 R. Valiente and F. Rodriguez, *J. Phys.: Condens. Matter*, 1998, **10**, 9525.
71 M. J. Llopis, G. Alzuet, A. Martin, J. Borrás, S. Garía-Grands and R. Días, *Polyhedron*, 1993, **12**, 3881.
72 G. Hanson, *XSophe, "A Professional CW EPR Computer Simulation Software Suite", Version 1.1.4.3*, 2007.
73 X-Area, STOE, Darmstadt, 2004.
74 G. M. Sheldrick, *SHELXS-97, Program for the Solution of Crystal Structures, Göttingen*, 1997.
75 G. M. Sheldrick, *SHELXS-97, Program for the Refinement of Crystal Structures, Göttingen*, 1997.
76 *"DIAMOND–Crystal and Molecular Structure Visualization", Program Version 3.1*, Crystal Impact, 2005.
77 M. J. Frisch, G. W. Trucks, H. B. Schlegel, G. E. Scuseria, M. A. Robb, J. R. Cheeseman, G. Scalmani, V. Barone, B. Mennucci, G. A. Petersson, H. Nakatsuji, M. Caricato,

 This journal is © The Royal Society of Chemistry and the Centre National de la Recherche Scientifique 2011

View Article Online

Published on 05 October 2011. Downloaded by TU Berlin - Universitaetsbibl on 31/03/2016 12:42:47.

X. Li, H. P. Hratchian, A. F. Izmaylov, J. Bloino, G. Zheng, J. L. Sonnenberg, M. Hada, M. Ehara, K. Toyota, R. Fukuda, J. Hasegawa, M. Ishida, T. Nakajima, Y. Honda, O. Kitao, H. Nakai, T. Vreven, J. A. Montgomery, Jr., J. E. Peralta, F. Ogliaro, M. Bearpark, J. J. Heyd, E. Brothers, K. N. Kudin, V. N. Staroverov, R. Kobayashi, J. Normand, K. Raghavachari, A. Rendell, J. C. Burant, S. S. Iyengar, J. Tomasi, M. Cossi, N. Rega, J. M. Millam, M. Klene, J. E. Knox, J. B. Cross, V. Bakken, C. Adamo, J. Jaramillo, R. Gomperts, R. E. Stratmann, O. Yazyev, A. J. Austin, R. Cammi, C. Pomelli, J. W. Ochterski, R. L. Martin, K. Morokuma, V. G. Zakrzewski, G. A. Voth, P. Salvador, J. J. Dannenberg, S. Dapprich, A. D. Daniels, O. Farkas, J. B. Foresman, J. V. Ortiz, J. Cioslowski and D. J. Fox, *Gaussian 09, Revision A.02*, Gaussian, Inc., Wallingford, CT, 2009.

78 G. W. Trucks, T. A. Keith and M. J. Frisch, *J. Chem. Phys.*, 1996, **104**, 5497.

79 M. R. Sunberg, R. Kikevaes, J. Ruiz, J. M. Moreno and E. Colacio, *Inorg. Chem.*, 1992, **31**, 1062.

80 S. Keinan and D. Avnir, *Inorg. Chem.*, 2001, **40**, 318.

81 S. Keinan and D. Avnir, *J. Chem. Soc., Dalton Trans.*, 2001, 941.

82 J. Cirera, P. Alemany and S. Alvarez, *Chem.–Eur. J.*, 2004, **10**, 190.

83 J. Tomasi, B. Mennucci and R. Cammi, *Chem. Rev.*, 2005, **105**, 2999.

84 L. Subramanian and R. Hoffmann, *Inorg. Chem.*, 1992, **31**, 1021.

85 C. H. Arnby, S. Jagner and I. Dance, *CrystEngComm*, 2004, **6**, 257.

86 B. N. Figgis and M. A. Hitchman, *Ligand Field Theory and its Application*, Wiley-VCH, New York, 2000.

87 H. Place and R. D. Willett, *Acta Crystallogr., Sect. C: Cryst. Struct. Commun.*, 1987, **43**, 1050.

88 U. Geiser and R. D. Willett, *Croat. Chem. Acta*, 1984, **57**, 737.

89 R. L. Harlow and W. J. Wells, *Inorg. Chem.*, 1974, **13**, 2106.

90 J. F. Stoddart, *Chem. Brit.*, 1991, 714.

91 B. J. Hathaway and D. E. Billing, *Coord. Chem. Rev.*, 1970, **5**, 143.

92 H. Yokoi and A. W. Addison, *Inorg. Chem.*, 1977, **16**, 1341.

93 B. Wenzel, U. Drutkowski and P. Strauch, *Z. Anorg. Allg. Chem.*, 2001, **627**, 973.

94 J. R. Wasson, H. W. Richardson and W. E. Hatfield, *Z. Naturforsch., B: Anorg. Chem., Org. Chem.*, 1977, **32**, 551.

95 A. Bencini, D. Gatteschi and C. Zanchini, *J. Am. Chem. Soc.*, 1980, **102**, 5234.

96 V. I. Murav'ev, *Russ. J. Coord. Chem.*, 2005, **31**, 643.

97 V. I. Murav'ev, *Russ. J. Coord. Chem.*, 2005, **31**, 206.

98 T. M. Kite and J. E. Drumheller, *J. Magn. Reson.*, 1983, **54**, 253.

99 R. D. Willett and R. J. Wong, *J. Magn. Reson.*, 1981, **42**, 446.

100 R. D. Willett, R. Wong and M. Numata, *J. Magn.Magn. Mater.*, 1980, **15–18**, 717.

101 R. D. Willett, R. J. Wong and M. Numata, *Inorg. Chem.*, 1983, **22**, 3189.

102 A. Bencini and D. Gatteschi, *J. Am. Chem. Soc.*, 1983, **105**, 5535.

103 K. Thiel, T. Klamroth, P. Strauch and A. Taubert, *Phys. Chem. Chem. Phys.*, 2011, **13**, 13537.